



Spectro polarimetry with liquid crystals

J.-M. Malherbe¹, Th. Roudier², J. Moity¹, P. Mein¹, J. Arnaud³, and R. Muller²

¹ Observatoire de Paris, LESIA, 92195 Meudon Cedex, France (e-mail: Jean-Marie.Malherbe@obspm.fr)

² Observatoire Midi Pyrénées, 57 Avenue d'Azereix, BP826, 65008 Tarbes, France

³ Observatoire Midi Pyrénées, 14 Avenue Edouard Belin, 31400 Toulouse, France

Abstract. We report spectro polarimetric observations made with the spectrograph of the Lunette Jean Rösch at Pic du Midi, France. We have tested Ferroelectric (FLC) and Nematic (NLC) Liquid Crystals. The instrument setup is briefly described, together with first observations of magnetic fields obtained with the Multichannel Subtractive Double Pass (MSDP). Polarization analysis of various spectral lines performed with the single pass (SP) spectrograph in active regions or at the limb is also presented.

Key words. Sun: atmosphere – Sun: magnetic fields

1. Introduction

The Pic du Midi 50 cm refractor is well known for high resolution images of the solar granulation obtained in the past. As the beam has an axial symmetry, instrumental polarization is minimized, therefore spectro polarimetry is possible with the spectrograph built in the eighties by Paris Observatory. High resolution observations with good seeing need short exposure times (ms), which are not compatible with a good signal to noise (S/N) ratio. For that reason, a large number of images must be acquired in a short time, which requires a fast observing cadence. For that purpose, we decided to use liquid crystals which have very short switching times between two states of polarization. The scientific goals are the determination of intense magnetic fields with good spatial resolution in the quiet sun and active regions (Zeeman effect) and weak, turbulent and

unresolved fields at the limb (Hanle depolarization).

2. Experiment setup

We used the D=50 cm refractor of Pic du Midi (primary focus $F1 = 6.5$ m) in combination with the 8 m Littrow Echelle spectrograph (316 grooves/mm) designed by Mouradian et al (1980). We started in 2003 the construction of a FLC polarimeter which was followed in 2004 by a more sophisticated version using NLC variable retarders. The polarimeter is located at focus $F1$ ($F1/D=13$). Image is then magnified 10 times to form at focus $F2$ ($F2/D=130$) on the entrance slit of the spectrograph (typical dispersion of 50 mm per nm). On exit, the spectrum (60 mm x 90 mm) is reduced 10 times to form on a low noise 1376 x 1040 x 12 bits CCD detector (4 e of readout noise at 16 MHz, 20000 e full well capacity, 4 e/ADU). The grating orders (typically 8 - 15) are selected by interference filters (10 nm bandwidth).

Send offprint requests to: J.-M. Malherbe

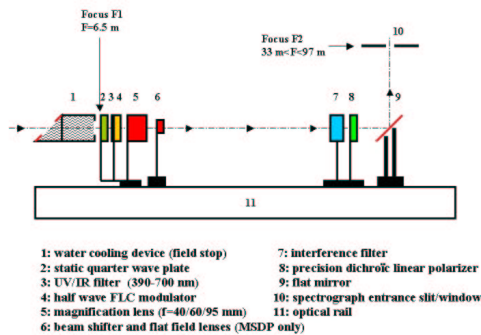


Fig. 1. The FLC polarimeter (optical rail between F1 and F2).

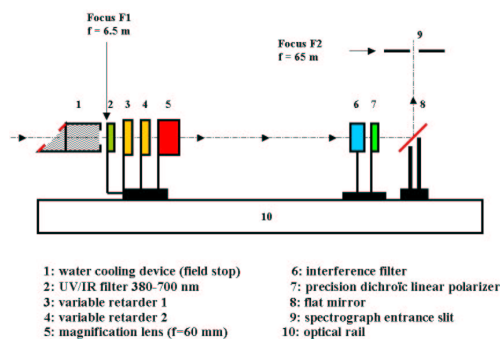


Fig. 2. The NLC polarimeter (optical rail between F1 and F2).

The FLC polarimeter, as shown in Fig. 1, is a half wave modulator (from Displaytech, USA). It provides the signal $S = \frac{1}{2}(I + Q \cos \delta - V \sin \delta)$, where I , Q , U and V are the Stokes parameters (in our reference frame Q characterizes the polarization parallel to the limb) and δ is the retardance of the crystal (approximately 0 or π , so that it will deliver $I \pm Q$ with a little cross talk from V). $I \pm V$ can also be measured in combination with a static quarter wave plate. The FLC is very fast (10 KHz), but presents some chromatism. The modulation is driven by a DC current ($\pm 5V$) to switch from 0 to half wave in the visible range 400 - 700 nm (see Fig. 3).

The NLC polarimeter, presented in Fig. 2 is more powerful and precise. It uses 2 variable retarders (from Meadowlark, USA) and allows

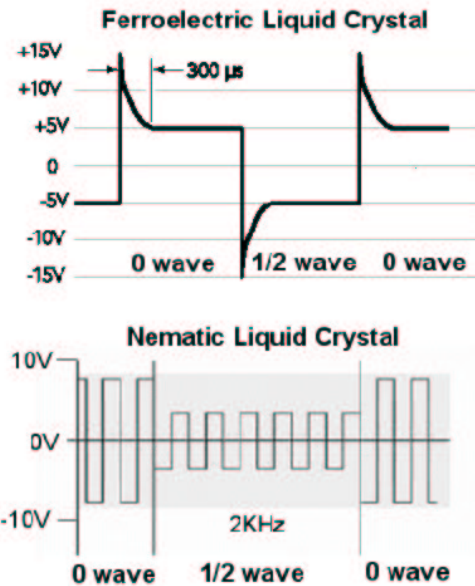


Fig. 3. Modulation technique with FLC (top) and NLC (bottom) polarimeters.

full Stokes polarimetry, at a moderate speed (40 Hz). The driving signal is a 2 KHz square wave (Fig. 3), with variable amplitude between 0 to 10 V, so that the retardance is continuously adjustable in the range 0 - 600 nm (0 to $3\lambda/4$ in the visible range). Hence, the NLC has no chromatism. It was calibrated in laboratory using interference filters for 17 spectral ranges (Fig. 4). The signal S provided by the NLC polarimeter is given by $S = \frac{1}{2}(I + Q \cos \delta_2 + \sin \delta_2(U \sin \delta_1 - V \cos \delta_1))$, where δ_1 and δ_2 are the variable retardances of the two crystals. In practice, the observing cadence is limited by the throughput of the detector (10 Hz) and exposure time values to achieve a typical S/N ratio of 100 for each pixel of the frame. In order to increase the S/N ratio, one has to take and combine several successive images. For more details, please refer to Malherbe et al (2006).

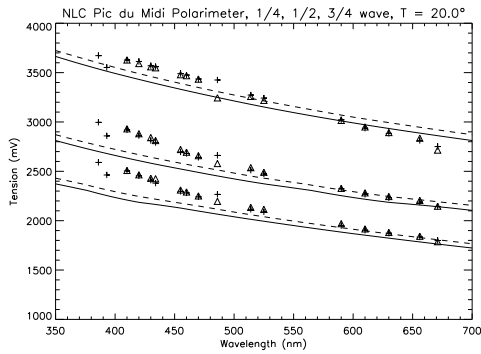


Fig. 4. Calibration of the 2 variable retarders (crosses and triangles): the voltage to apply for $\lambda/4$ (top), $\lambda/2$ (middle) and $3\lambda/4$ (bottom) retardance at various wavelengths (386, 393, 410, 420, 430, 434, 455, 460, 470, 486, 514, 523, 590, 610, 630, 656 and 670 nm). The two curves (for comparison) were provided by the manufacturer.

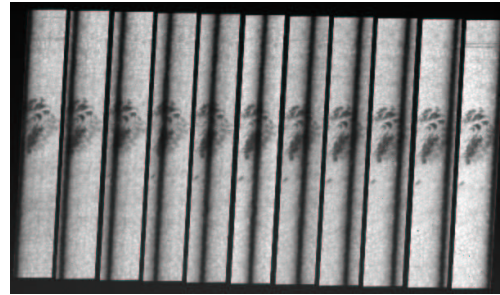


Fig. 5. MSDP image with 11 channels in NaDI 589.6 nm line. FOV $20'' \times 150''$.

3. Solar surface magnetometry

3.1. MSDP mode

The MSDP spectrograph (Mein, 1977, 2002) allows observations over a 2D field of view of line profiles as NaDI 589.6 nm using 11 simultaneous channels with good spatial ($0.3''$) and temporal resolutions (Fig. 5). Malherbe et al (2004) and Roudier et al (2006) performed observations of magnetic fields in an active region. We present here the data obtained with the FLC polarimeter (Fig. 6) by Malherbe et al (2004). Radial Velocities ($V_{||}$) and magnetic fields ($B_{||}$) are derived from the wavelength shifts determined by the bisector method. We detect the position in wavelength of the middle of a chord of half width $\Delta\lambda$. If λ_1 is the reference position (quiet sun) and λ_2 the current position, $(\lambda_1 + \lambda_2)/2$ is proportional to $V_{||}$ (Doppler shift) and $(\lambda_1 - \lambda_2)/2$ to $B_{||}$ through the Landé factor (Zeeman shift, weak field approximation). We used two positions: $\Delta\lambda=14.4$ pm for the low chromosphere and $\Delta\lambda=28.8$ pm for the high photosphere (altitude difference of 160 km). Fig. 6b shows the high altitude field $B_{||}$ derived from a single pair of $I \pm V$ images with a noise of 60 G, while Fig. 6c has a noise of only 25 G because 10 pairs of $I \pm V$ images were aligned, distretched and summed to in-

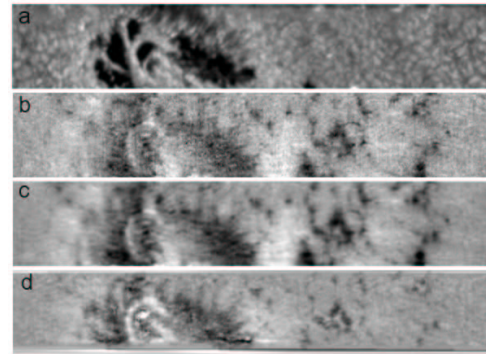


Fig. 6. a: NaDI continuum intensity. b: magnetic fields $B_{||}$ derived from one pair of $I \pm V$ images, at $\Delta\lambda = 14.4$ pm. c: $B_{||}$ derived from 10 pairs of $I \pm V$ images at $\Delta\lambda = 14.4$ pm (high altitude). d: $B_{||}$ derived from 10 pairs of $I \pm V$ images at $\Delta\lambda = 28.8$ pm (low altitude).

crease the S/N ratio. Fig. 6d is the low altitude field based on 10 pairs of $I \pm V$ images. The field of view (FOV) is $15'' \times 90''$.

Fig. 7 shows a detail of the quiet area located right of the sunspot (FOV $15'' \times 40''$). On this area, we found that magnetic concentrations are mainly located in intergranular lanes and have a mean field strength of 420 G and a mean downward velocity of 590 m/s at $\Delta\lambda = 14.4$ pm (respectively 630 G and a downward velocity of 950 m/s at $\Delta\lambda = 28.8$ pm). Velocities and magnetic fields were found to decrease as a function of altitude. Roudier et al (2006) and Mein et al (2006) found that this is not always the case.

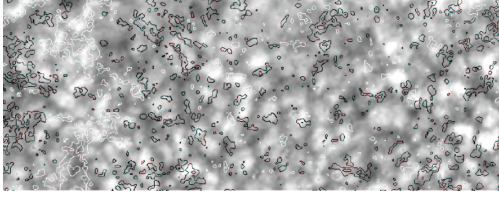


Fig. 7. NaD1 589.6 nm continuum intensity and isocontours of $B_{//}$.

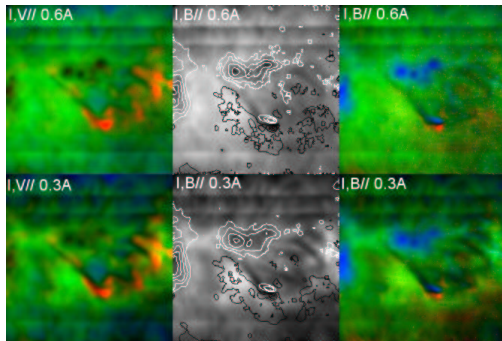


Fig. 8. $H\alpha$ dopplergrams (left) and magnetograms (middle and right) for two altitudes at $\Delta\lambda = 60\text{pm}$ (top) and $\Delta\lambda = 30\text{pm}$ (bottom). The background represents intensities.

Chromospheric magnetic fields were also investigated for JOP178 with the MSDP in $H\alpha$ 656.3 nm, as shown in Fig. 8 where dopplergrams and magnetograms were calculated at two different altitudes over an active region (FOV $2' \times 2'$) and superimposed on intensities. In order to improve the S/N ratio, real time accumulation of 8 pairs of $I \pm V$ images was performed, this procedure is convenient when the spatial resolution is moderate. The time resolution was excellent (2 mn): observations in MSDP mode are well suited for rapidly evolving phenomena.

3.2. Chromospheric lines in SP mode

The SP spectroscopic mode allows to have a better spectral resolution (typically 1.5 pm) than the MSDP (15 pm for NaD1 at Pic du Midi, 8 pm at THEMIS), but the FOV is only 1D (thin slit). We present now two preliminary observations made with the NLC polarimeter.

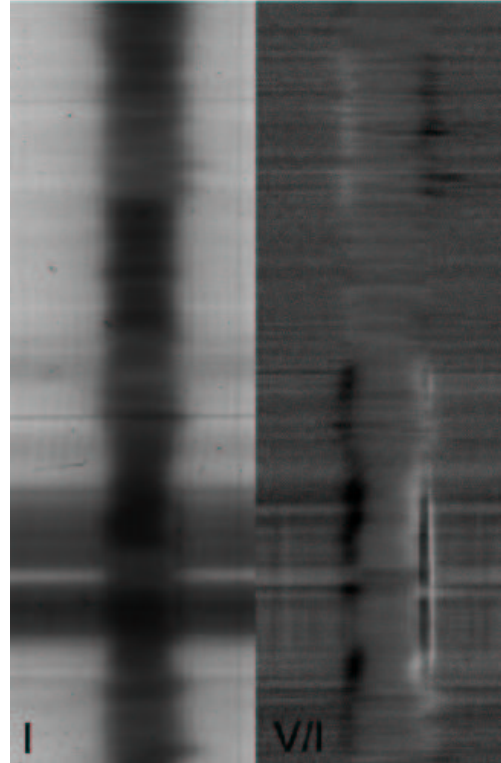


Fig. 9. $H\alpha$ 656.3 nm intensities (left) and Stokes V/I (right). In abscissa: the wavelength; in ordinates: the solar direction.

We observed, as shown by Fig. 9, $H\alpha$ line profiles in Stokes V over an active region. A blend appears just in the sunspot in the red wing of the line. This is the CoI 656.34 nm line, already noticed by Balasubramaniam et al (2004), which inhibits good determination of the magnetic field in the umbra of sunspots. On the contrary, this blend does not appear in quiet areas or in faculae. Exposure times are a few tens of ms with a slit of $0.3''$.

Fig. 10 shows the CaII K 393.3 nm line in the near UV over an active region (sunspot, faculae). It is a difficult line to observe because exposure times are long (1 s with a slit of $1''$). For this line, the grating order is high so that the spectral pixel is only 0.93 pm. As noticed by Mattig and Kneer (1978), the line core has a strong emission in the sunspot umbra. The Zeeman effect is very obvious, but it is reversed

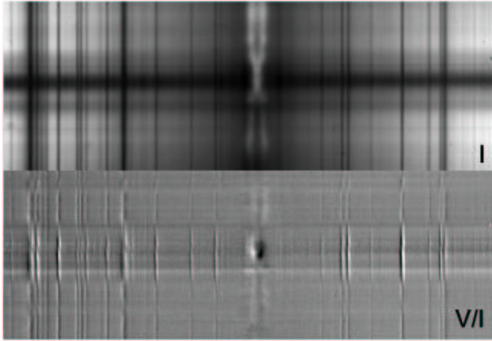


Fig. 10. CaII K 393.3 nm intensities (top) and Stokes V/I (bottom). In abscissa: the wavelength; in ordinates: the solar direction. The spectral range from left to right is 1.2 nm.

in comparison to other lines as FeI of the spectral domain. The FOV is $90''$.

4. Stokes Q of the second solar spectrum

The second solar spectrum is the linearly polarized spectrum observed at the limb of the sun. It is as rich as the ordinary intensity spectrum, but the two spectra are very different. The second solar spectrum is generated by coherent scattering due to the anisotropy of the radiation field, both with and without magnetic fields. The polarization rate is generally small (1% or less) and decreases in the presence of magnetic fields. This well known effect is called Hanle depolarization and is often observed in Stokes Q/I, which characterizes the linear polarization parallel to the limb. The measure of the depolarization of spectral lines allows to derive the strength of weak, non resolved and turbulent magnetic fields in the solar photosphere. We started this program in 2003.

4.1. Polarimetric spectroscopy of the limb

Fig. 11 presents some results obtained in October 2006 with the FLC polarimeter at various distances of the limb of the polarization of SrI 460.7 nm line. The slit was parallel to the South limb. Data were averaged along the

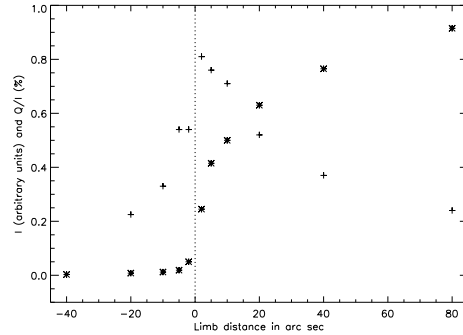


Fig. 11. Centre to limb variation of the linear polarization of SrI 460.7 nm. Crosses (+) for Q/I and stars (*) for intensities. In abscissa: limb distance (negative means above the limb). The dotted line indicates limb position.

slit ($140''$). Limb distances are negative above the limb ($-40''$, $-20''$, $-10''$, $-5''$, $-2''$) and positive on the disk ($2''$, $\mu = 0.06$; $5''$, $\mu = 0.1$; $10''$, $\mu = 0.15$; $20''$, $\mu = 0.2$; $40''$, $\mu = 0.3$; and $80''$, $\mu = 0.4$). Above the limb, we observed scattered light around the sun; we noticed that, despite of the intensity drop (exposure times were increased to keep the same S/N ratio), linear polarization surprisingly remains high. Other results with the NLC polarimeter concerning SrI 460.7 nm, BaII 455.4 nm, CaI 422.7 nm and NaD1 589.6 nm have been recently published (Malherbe et al, 2006).

4.2. polarimetric imagery of the limb with filters

Fig. 12 shows the linear polarisation Q/I integrated over a 10 nm bandwidth centered at 410 nm and 470 nm. In the blue part of the spectrum, the continuum polarization of the limb is high and can be measured in imagery mode. But it requires filters 10 times more narrow than the one we used to isolate a clean portion of the spectrum, to avoid polarization or depolarization of the continuum by spectral lines. However, this result demonstrates the capability of our instrument to measure the continuum polarization.

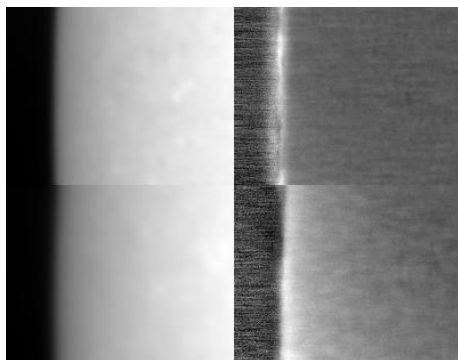


Fig. 12. Intensity I (left) and linear polarization Q/I of the limb (right) at 410 nm (bottom) and 470 nm (top).

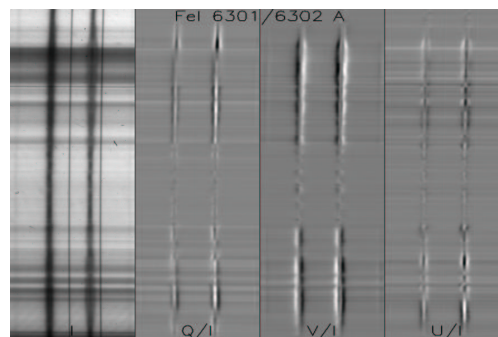


Fig. 13. Full Stokes spectro polarimetry (I , Q/I , V/I , U/I) of FeI 630.15 and 630.25 nm lines. In abscissa: the wavelength; in ordinates: the solar direction.

5. Full Stokes spectro polarimetry

With the NLC polarimeter, it is possible to perform observations in full Stokes polarimetry in SP mode. The spectral resolution of the multi slit beamshifter of the MSDP is not enough at Pic du Midi to record the Stokes vector. As we do not have the possibility to scan the solar surface in SP mode, we had to keep the slit in a fixed position on the sun. We give two examples of spectral lines which were recorded over an active region with two opposite polarities in order to show the capabilities of the instrument. It will be possible to scan the solar surface in the fall of 2007 after some mechanical improvements concerning the equatorial mount of the refractor. The FOV is about $140''$.

Fig. 13 shows the classical lines of FeI 630.15 nm and 630.25 nm usually used by magnetographs (THEMIS, Solar B Hinode) to produce vector magnetograms. Fig. 14 shows the FeI 525.02 nm and 525.07 nm lines.

6. Conclusions

We have shown that Nematic Liquid Crystals allow fast polarimetry with no chromatism for sequential observations of spectral lines. A beam splitter shifter will be incorporated soon in order to observe simultaneously pairs of signals $I \pm P$, where P is any Stokes parameter. Beam exchange will be easily available.

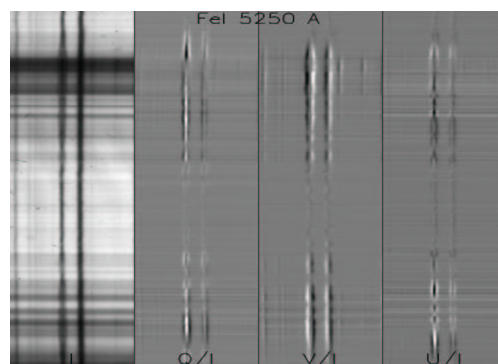


Fig. 14. Full Stokes spectro polarimetry (I , Q/I , V/I , U/I) of FeI 525.02 and 525.07 nm lines. In abscissa: the wavelength; in ordinates: the solar direction.

We have presented high resolution observations of magnetic fields in the quiet sun with the MSDP device, and measurements of the second solar spectrum with the SP spectrograph.

Our instrument has a good sensitivity in the blue part of the spectrum (390 - 460 nm) and allows observations at high spatial resolution ($0.3''$). It will be used for observations which cannot be done with THEMIS.

Acknowledgements. We are indebted to Ch. Coutard, engineer in optics, for his help in the optical setup of the experiment and his support during the observations. The spectrograph was designed by Z. Mouradian. This work was sup-

ported by Observatoire de Paris, Observatoire Midi Pyrénées, CNRS (UMR 8109 and UMR 5572) and the Programme National Soleil Terre (PNST).

References

- Balasubramaniam, K. S., Christopoulou, E. B., Uitenbroeck, H., 2004, *ApJ*, 606, 1233
- Malherbe, J.-M., Roudier, Th., Mein, P., Moity, J., Muller, R., 2004, *A&A*, 427, 745
- Malherbe, J.-M., Moity, J., Arnaud, J., Roudier, Th., 2006, *A&A*, in press
- Mattig, W., Kneer, F., 1978, *A&A*, 65, 11
- Mein, P., 1977, *Solar Physics*, 54, 45
- Mein, P., 2002, *A&A*, 381, 271
- Mein, P., Mein, N., Faurobert, M., Aulanier, G., Malherbe, J.-M., 2006, *A&A*, in press
- Mouradian, Z., Chauveau, F., Colson, F., Darre, G., Kerlirzlin, P., Olivieri, G., 1980, *Japan France Seminar on Solar Physics*, 271
- Roudier, T., Malherbe, J.M., Moity, J., Mein, P., Coutard, C., 2006, *A&A*, 455, 1091